Available online at www.sciencedirect.com
ScienceDirect
Biochimica et Biophysica Acta 1768 (2007) 2355–2364
Biochimica et Biophysica Acta
BBA
www.elsevier.com/locate/bbamem

Solution structures and model membrane interactions of lactoferrampin, an antimicrobial peptide derived from bovine lactoferrin

Evan F. Haney, Fanny Lau, Hans J. Vogel *

Structural Biology Research Group, Department of Biological Sciences, University of Calgary, Calgary, Alberta, Canada T2N 1N4

Received 21 February 2007; received in revised form 15 April 2007; accepted 20 April 2007
Available online 1 May 2007

Abstract

Bovine lactoferrampin (LFampinB) has been identified as a novel antimicrobial peptide, which is derived from the N-terminal lobe of bovine lactoferrin. In this study, the solution structure of LFampinB bound to negatively charged sodium dodecyl sulphate micelles and zwitterionic dodecyl phosphocholine micelles was determined using 2-dimensional nuclear magnetic resonance (NMR) spectroscopy. The interaction between LFampinB and multilamellar phospholipid vesicles, containing choline and glycerol head groups, was examined using differential scanning calorimetry (DSC). In addition, the interaction between the N-terminal tryptophan residue and model membranes of varying composition was analyzed by fluorescence spectroscopy. LFampinB adopts an amphipathic alpha-helical conformation across the first 11 residues of the peptide but remains relatively unstructured at the C-terminus. The hydrophobic surface of the amphipathic helix is bordered by the side chains of Trp1 and Phe11, and is seen in both micelle-bound structures. The fluorescence results suggest that Trp1 inserts into the membrane at the lipid/water interface. The phenyl side chain of Phe11 is oriented in the same direction as the indole ring of Trp1, allowing these two residues to serve as anchors for the lipid bilayer. The DSC results also indicate that LFampinB interacts with glycerol head groups in multilamellar vesicles but has little effect on acyl chain packing. Our results support a two step model of antimicrobial activity where the initial attraction of LFampinB is mediated by the cluster of positive charges on the C-terminus followed by the formation of the N-terminal helix which binds to the surface of the bacterial lipid bilayer.

Keywords: Antimicrobial peptide; Lactoferrampin; Lactoferrin; Nuclear magnetic resonance; Micelle-bound peptide structure; Peptide–membrane interactions

1. Introduction

The emergence of antibiotic resistant pathogenic bacteria has triggered a need to discover novel antimicrobial agents. Antimicrobial peptides are naturally occurring molecules that have shown promise as effective antimicrobial agents. Some antimicrobial peptides are fragments of larger proteins that display higher activity when proteolytically cleaved from the parent molecule. Examples of these are lactoferricins which are cleaved from lactoferrin [1,2] and peptides derived from the proteolysis of lysozyme [3,4]. Recent research into antimicrobial peptides has led to the identification of novel antimicrobial sequences that are found within proteins that are not naturally cleaved by proteases.

One novel antimicrobial peptide sequence was recently discovered in bovine lactoferrin and the resulting synthetic peptide was termed lactoferrampin [5]. Lactoferrin is an 80 kDa iron binding protein that has been implicated in numerous functions ranging from antibacterial activity to stimulation of the immune system [6]. Most of the activity of lactoferrin has been attributed to the highly cationic N-terminal region of the protein. Lactoferricin is an antimicrobial peptide derived from this region that is released through pepsin hydrolysis of lactoferrin under acidic conditions [1]. This peptide fragment possesses a wide variety of biological activities including, antimicrobial, antiviral

Abbreviations: LFampinB, bovine lactoferrampin; NOESY, nuclear Overhauser effect spectroscopy; TOCSY, total correlation spectroscopy; DPC, dodecylphosphocholine; SDS, sodium dodecylsulfate; DSS, 2,2-dimethyl-2-silapentane-5-sulphonic acid; ePC, egg α-phosphatidylcholine; ePG, egg α-phosphatidylglycerol; ePE, egg α-phosphatidylethanolamine; PA, phosphatidic acid; MLV, multilamellar vesicle; LUV, large unilamellar vesicle; K_{sv}, Stern–Volmer constant; MIC, minimum inhibitory concentration; MBC, minimum bactericidal concentration; DPPC, 1,2-dipalmitoyl phosphatidylcholine; DPPG, 1,2-dipalmitoyl phosphatidylglycerol; DSC, differential scanning calorimetry

* Corresponding author. Tel.: +1 403 220 6006; fax: +1 403 289 9311.
E-mail address: vogel@ucalgary.ca (H.J. Vogel).

0005-2736/$ - see front matter © 2007 Elsevier B.V. All rights reserved.
doi:10.1016/j.bbamem.2007.04.018

and immunological properties and in some cases these activities are more potent than the intact lactoferrin protein [7]. Many synthetic peptides modeled after this sequence have been examined to determine the mechanism of antimicrobial action of this peptide [8–10]. Bovine lactoferrampin (LFampinB) corresponds to residues 268–284 of bovine lactoferrin and is also found in the cationic N-terminal lobe of lactoferrin [5]. This fragment was identified as a potential antimicrobial sequence because it possessed many attributes characteristic of other known antimicrobial peptides, such as the presence of a tryptophan residue and a net cationic charge [11,12]. LFampinB was shown to have antimicrobial activity against both Gram positive and Gram negative bacteria as well as *Candida albicans* [5].

In spite of the increasing number of antimicrobial peptides that are being identified, the mechanism of action for many of these peptides remains unclear. The majority of antimicrobial peptides are believed to act upon the bacterial membrane by making them leaky, punching holes through them or completely solubilizing them [13]. An important aspect of determining the mode of action employed by an antimicrobial peptide is to study its ability to interact with membranes and to determine the solution structure of peptides bound to membrane mimetic micelles. This can provide valuable insight into the distribution of the charges on the surface of the peptide and allows one to examine if the structure is amphipathic, a characteristic feature of many antimicrobial peptides [14]. The solution structure of these antimicrobial peptides bound to lipid micelles can be extended to predict the interaction between the peptide and the membrane surfaces of microbes and lends support to certain models of the mode of action used to kill bacterial cells. To date the only structural information available for LFampinB is a circular dichroism study in which it was found that the LFampinB has a mixture of helical and disordered regions [15].

Here we present the solution structures of bovine lactoferrampin bound to negatively charged sodium dodecyl sulfate (SDS) micelles and zwitterionic dodecylphosphocholine (DPC) micelles. Furthermore, we characterize the interaction of the N-terminal Trp residue with large unilamellar vesicles of varying phospholipid composition. Additionally, we examine the interaction between LFampinB and multilamellar vesicles using differential scanning calorimetry. An amphipathic helical structure with a disordered C-terminus is seen in the micelle-bound structures of LFampinB determined by NMR spectroscopy. Our results indicate that LFampinB interacts with vesicles containing phospholipids with negatively charged head groups, while this interaction is not evident in the presence of zwitterionic vesicles.

2. Materials and methods

2.1. Synthesis of peptides and materials used

Bovine lactoferrampin (WKLLSKAQEKFGKNKSR) was purchased from Anaspec, Inc. (San Jose, CA) and obtained at a purity of >95%. This sequence of LFampinB corresponds directly to that used in the original experiments reported for this peptide [5]. Peptide concentrations were determined using a theoretical extinction coefficient of ε(280) 5500 M^{-1} cm^{-1}.

All phospholipids were obtained from Avanti Polar Lipids (Alabaster, AL) except for sodium dodecyl sulphate (SDS) which was obtained from EMD Chemicals Inc. (Gibbstown, NJ). The phospholipids used in the preparation of LUVs were egg α-phosphatidylglycerol (ePG), egg α-phosphatidylethanolamine (ePE) and egg α-phosphatidylcholine (ePC). Deuterated SDS and DPC used in the NMR samples were obtained from CDN Isotopes (Pointe-Claire, QC, Canada).

1,2-dipalmitoyl phosphatidylglycerol (DPPG) and 1,2-dipalmitoyl phosphatidyl choline (DPPC) were obtained from Avanti Polar lipids as sodium salts (purity>99%) and were used without further purification.

2.2. Vesicle preparation

Large unilamellar vesicles (LUVs) were prepared according to the protocol described by Schibli et al. [16]. LUVs were prepared from 1:1 mixtures of ePC:ePG, ePC:ePE and ePE:ePG lipids. Lipid films were prepared by evaporating the chloroform solvent from the lipid mixtures under a stream of nitrogen followed by incubation under a vacuum for 1.5 h. The lipid film was resuspended in Tris buffer (10 mM Tris, 150 mM NaCl, 1 mM EDTA, pH 7.4) and vortexed. The lipid suspensions were subjected to five rounds of freezing in liquid nitrogen and thawing, followed by 15 passes through two 0.1 μm polycarbonate filters (Nucleopore Filtration Products, Pleasonton , CA) using a mini-extruder apparatus (Avanti Polar Lipids) at room temperature [17,18]. The concentration of lipid in the LUV samples was determined using the Ames method [19] which determines the phosphorus concentration within the sample. The phosphorus concentration in the buffer was determined and subtracted from the samples containing LUVs.

Multilamellar vesicles used in the DSC experiments were prepared according to the protocol outlined by Prenner et al. [20]. Stock solutions of DPPG and DPPC were prepared by dissolving the solid powder in pure methanol. The LFampinB stock solution was also prepared in methanol. All of the lipid:peptide ratios were prepared using the stock solutions of lipid and peptide in methanol and then lipid films were achieved by evaporating the organic solvent under a stream of nitrogen. The lipid films were then placed under a vacuum overnight to remove any remaining methanol. Lipid films and buffer were heated to approximately ten degrees above the phase transition temperature then the lipid film was hydrated with the heated buffer. Samples were vortexed to ensure full lipid mixing. All the MLV samples were prepared in 20 mM phosphate buffer, containing 130 mM NaCl at pH 7.4.

2.3. Fluorescence

Fluorescence measurements were performed on a Varian Cary Eclipse fluorimeter (Varian Inc. Palo Alto, CA.) equipped with a temperature control unit, set at 20 °C, and a multi-cell sample holder. Emission spectra were obtained between 300 nm and 500 nm using an excitation wavelength of 280 nm. The slit width for the excitation light was 10 nm except for the samples containing DPC, where the emission spectra of the Trp fluorophore was significantly higher and the slit width was adjusted to 5 nm to accommodate the increase in intensity. The slit width of the emission settings was maintained at 10 nm throughout all the experiments. Spectra were collected on a 2-mL sample of 1 μM peptide in Tris buffer at pH 7.4. In these experiments, the following membrane mimetic environments were tested: 30 μM ePC:ePG LUVs, 30 μM ePC:ePE LUVs, 30 μM ePE:ePG LUVs, 25 mM SDS and 25 mM DPC.

In addition to measuring the intensity changes and blue shifts in the emission spectra of LFampinB, acrylamide quenching was performed on all of the peptide/lipid mixtures to calculate Stern–Volmer constants (K_{sv}) as previously done [16]. 5 μL aliquots of a 4.0 M stock acrylamide solution were added to the cuvette containing peptide and lipid. Emission spectra, as previously described, were collected after each addition of quencher up to a final acrylamide concentration of 0.1 M.

The K_{sv} [21] for each combination of LFampinB and lipid was calculated from the equation:

$$F_o/F = 1 + K_{SV}[Q]$$

where F_o is the initial fluorescence of the peptide and F is the fluorescence intensity following the addition of soluble quencher, Q.

2.4. Differential scanning calorimetry

DSC data were collected using a Microcal high-sensitivity VP-DSC (Microcal. Norhampton, MA). The total lipid concentration in all of the DSC experiments was

Table 1
Blue shift of tryptophan fluorescence in the presence of different membrane environments compared to the maximum emission wavelength of LFampinB in buffer

Membrane environment	Blue shift of the maximum wavelength (nm)
SDS	22
DPC	16
ePC:ePG LUVs	8
ePE:ePG LUVs	8
ePC:ePE LUVs	0
ePC LUVs	0

0.5 mg/mL. Lipid films containing peptide were prepared at lipid to peptide ratios of 100:1, 50:1 and 10:1. DPPC and DPPG were chosen as model lipids because of the 16 carbon fatty acyl chains that comprise a large proportion of the lipids found in biological membranes. Additionally the choline and glycerol head groups give a zwitterionic and negatively charged vesicle surface respectively. The 1,2-dipalmitoyl fatty acids also give well-defined transition peaks in the DSC thermograms in the temperature range tested. For all of the samples, a heating scan rate of 10 °C/h was used between 20 °C and 60 °C. All of the data acquisition and analysis was done using the Microcal Origin Software (version 7.0).

2.5. NMR samples

LFampinB was prepared in a 9:1 mixture of H_2O:D_2O to a concentration of 2.28 mM and a pH of 3.88. Once spectra were collected, deuterated SDS was added to this sample to a final concentration of 200 mM at a pH of 4.98. Another sample of LFampinB in the same ratio of H_2O and D_2O and 200 mM deuterated DPC was prepared with a peptide concentration of 1.04 mM and the pH was adjusted to 3.88. The acidic pH in all the NMR samples ensures a slow exchange of the amide protons with the aqueous solution. DSS was added as an internal standard to all the NMR samples to a final concentration of 0.2 mM.

2.6. NMR spectroscopy

Two-dimensional NOESY and TOCSY spectra were recorded at 298 K on a Bruker Avance 700 MHz spectrometer. NOESY mixing times were 500 ms for peptide samples in H_2O:D_2O and 100 ms for micelle bound samples. The mixing time in the TOCSY experiments was 120 ms. Spectra were obtained with 4096×600 data points in the F2 and F1 dimensions and a sweep width of 8992.806 Hz. Water suppression in the NOESY and TOCSY experiments was achieved using excitation sculpting [22]. All spectra were zero-filled and multiplied by a shifted sine-bell curve using the NMRPipe software package [23].

2.7. Structure calculations

Spectra were analyzed using NMRView 5.0.1.4 [24] running on a workstation using the Redhat 7.1 version of the Linux operating system. All spectra were referenced to DSS at 0.00 ppm. Proton chemical shifts were assigned according to Wuthrich [25]. Extended peptide structures were generated by CNS [26] and were used as a starting model for structure calculations. Dihedral angle restraints were placed upon all of the backbone angles of the peptide, except for Gly12, to start the dihedral angles of LFampinB in allowed regions of the Ramachandran plot. The structures were further refined by taking into account the unambiguous and ambiguous NOE restraints from the NOESY spectra using the program ARIA (version 1.2) [27]. In the final ARIA run, 100 structures were generated in the ninth iteration and the 20 lowest energy structures were kept and analyzed.

3. Results

3.1. Tryptophan fluorescence

Examining the change in fluorescence intensity and the shift in maximum emission wavelength of LFampinB provides information about the environment of the Trp fluorophore at the N-terminus of the peptide. A blue shift in the tryptophan fluorescence indicates that the fluorophore has moved into a hydrophobic environment, in this case the lipid tail region of the phospholipid bilayer. In addition, an increase in the intensity of the fluorescence indicates that the environment of the fluorophore has also changed from the peptide in buffer alone and that more of the energy from the excited state of the Trp side chain must escape as the emission of a photon as opposed to escaping through other non-radiative processes as it does in solution. This provides evidence to support the insertion of the N-terminal tryptophan residue into the hydrophobic core of the lipid bilayer.

The maximum emission wavelength of LFampinB in aqueous solution is 358 nm. It is assumed that this is the environment where the tryptophan residue is the most flexible and should have the highest emission wavelength. The largest blue shifts are observed in the presence of SDS and DPC micelles indicating a significant interaction between the peptide and the hydrophobic core of the lipids (Table 1). The blue shift in the presence of SDS micelles is larger than that observed in the presence of DPC micelles. This could be attributed to a stronger electrostatic attraction between the positively charged LFampinB peptide and the negatively charged SDS head groups.

When tested with LUVs of various composition, LFampinB interacted with ePC:ePG and ePE:ePG LUVs and not the ePC:ePE or ePC LUVs. It should be noted that these fluorescence experiments are not a direct measurement of peptide binding to the surface of the LUVs. However, there is a significant blue shift of the tryptophan fluorescence in the presence of ePG containing LUVs (Table 1) while there is no blue shift observed when LFampinB is mixed with zwitterionic LUVs composed of ePC:ePE or ePC alone (Table 1). These results suggest that LFampinB interacts with the surface of LUVs and that this interaction is favored by the presence of a negatively charged head group on the surface of the vesicle.

The maximum fluorescence intensity of Trp1 in LFampinB increased dramatically in the presence of DPC micelles, and it is for this reason that the excitation slit width had to be adjusted to

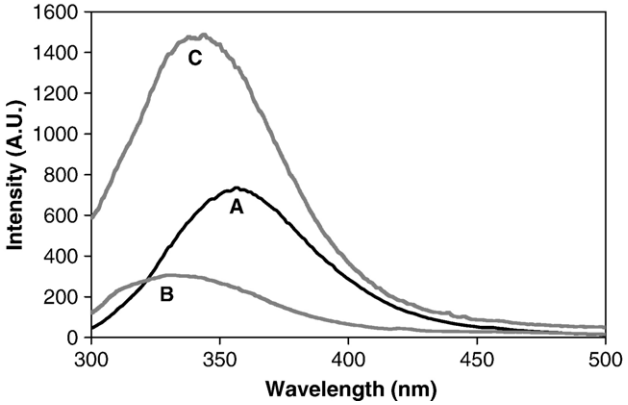

Fig. 1. Fluorescence emission of LFampinB in buffer (A) and in the presence of SDS (B) and DPC (C) micelles. Because the emission spectra of LFampinB bound to DPC micelles was collected using an emission wavelength of 5 nm compared to 10 nm used in the buffer and the SDS samples, the fluorescence intensity has been multiplied by a factor of 4.

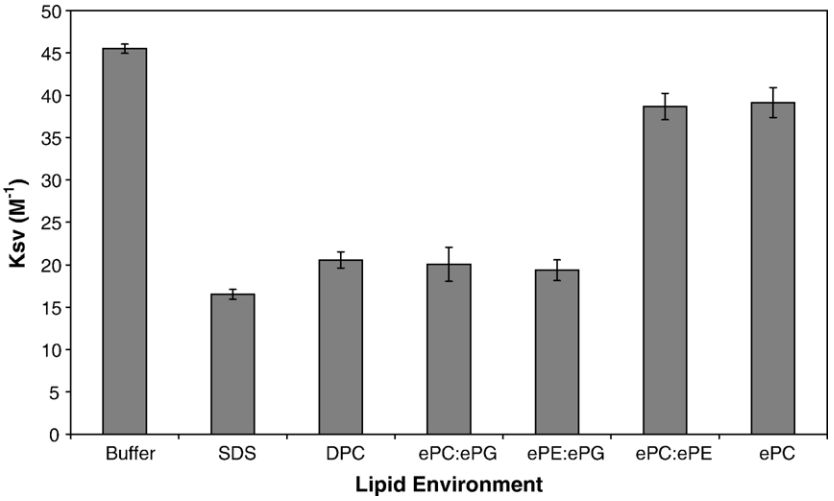

Fig. 2. Stern–Volmer constants calculated from the acrylamide quenching experiment for LFampinB in various membrane mimetic environments. All experiments were performed in triplicate.

bring the intensity within the range allowed for the fluorimeter (Fig. 1). Conversely, the emission spectra of LFampinB in the presence of SDS micelles had a lower intensity than the peptide in buffer (Fig. 1).

Determining the K_{sv} from the acrylamide quenching experiment provides more information about the extent to which the tryptophan is buried into the hydrophobic core of the lipid bilayer. As the Trp side chain embeds itself in the bilayer, it becomes less exposed to the surrounding solvent. This makes the fluorophore less susceptible to the effects of a neutral soluble quencher, such as acrylamide. A lower K_{sv} means a greater degree of protection of the Trp residue and indicates that the fluorophore is inserted into the hydrophobic core of the bilayer. Excess LUV and detergent was used to ensure that if an interaction between LFampinB and the lipid species occurred, all of the peptide in solution would have been in the lipid bound conformation and any contribution to the fluorescence from the free floating peptide would have been limited.

The K_{sv} for LFampinB in buffer was found to be $\sim 45\ M^{-1}$. In the presence of SDS, DPC, ePC:ePG and ePE:ePG, the K_{sv} is approximately half that value (Fig. 2). This indicates that the side chain of Trp1 has inserted itself into the lipid bilayer in these four membrane environments. This also supports the blue shifts observed for this peptide in the presence of these four lipid environments (Table 1). The K_{sv} of LFampinB mixed with ePC:ePE, and ePC LUVs is higher than the other lipid environments tested (Fig. 2). In fact it is closer to the values obtained for the free peptide in buffer indicating that the Trp residue is only weakly interacting with the LUV surface. The lack of a significant blue shift for LFampinB in these environments (Table 1) also demonstrates that the tryptophan residue at the N-terminus of LFampinB is in an environment similar to the peptide in buffer and that the peptide does not interact with the zwitterionic LUVs in the same manner as that observed with the negatively charged LUVs.

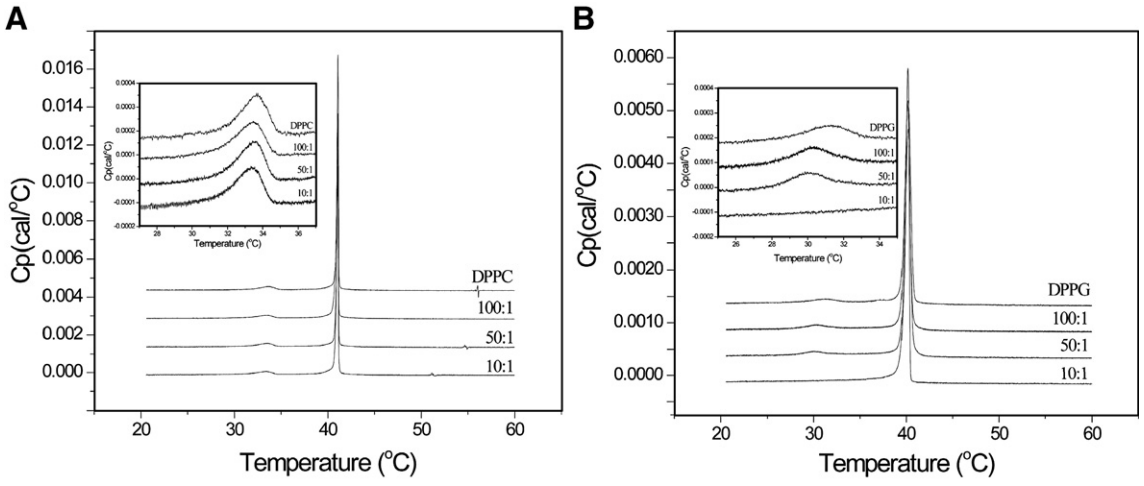

Fig. 3. Differential scanning calorimetry heating scans of DPPC (A) and DPPG (B) multilamellar vesicles and the effect of adding LFampinB to lipid:peptide ratios of 100:1, 50:1 and 10:1 as indicated on each figure. The pretransition region of the thermogram for each lipid species is shown as insets.

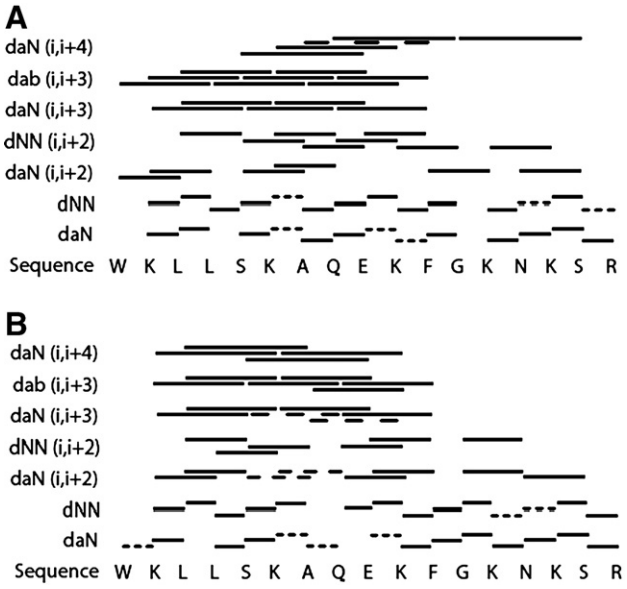

Fig. 4. NOE connectivities of LFampinB bound to SDS (A) and DPC (B) micelles. Unambiguous NOEs are represented by solid lines while ambiguous NOEs are shown as broken lines. Note that the majority of the NOEs contributing to the formation of a helical structure are found in residues at the N-terminal part (residues 1–11) of the peptide.

3.2. Differential scanning calorimetry

The DSC thermograms of LFampinB mixed with DPPC and DPPG MLVs are presented in Fig. 3. Increasing the concentration of LFampinB had no significant effect on the thermogram of DPPC MLVs. In the pure DPPC MLVs, a pretransition was observed at about 33.5 °C and main phase transition occurred at approximately 41 °C. These transitions can be found in all of the other heating scans at all of the lipid:peptide ratios tested with very little change in heat capacity or shape of the peak (Fig. 3A). In the case of pure DPPG MLVs, a pretransition occurs at approximately 31.5 °C with the main phase transition occurring at around 40 °C. The addition of LFampinB had a small effect on the phase behavior of DPPG MLVs. The pretransition at 31.5 °C shifted to lower temperatures with increasing LFampinB content until it disappears at a lipid:peptide ratio of 10:1 (Fig. 3B inset). Despite this effect on the pretransition, the main phase transition temperature of DPPG in the presence of LFampinB remained relatively unchanged (Fig. 3B).

3.3. NMR structures

LFampinB adopts a partial helical structure in the presence of SDS and DPC micelles at 298 K. Many of the distance restraints observed in the NOESY spectra of LFampinB in SDS and DPC are between amino acids in the first 11 residues of the peptide (Fig. 4). Characteristic (i,i+2; i,i+3; i,i+4) medium range NOEs for α-helical structures are found from residues 1 to 11. Because of the large number of NOE contacts in this region, a well-defined helical structure has been determined which encompasses residues 1–11 of LFampinB with the final 6 residues at the C-terminus remaining relatively unstructured (Fig. 5).

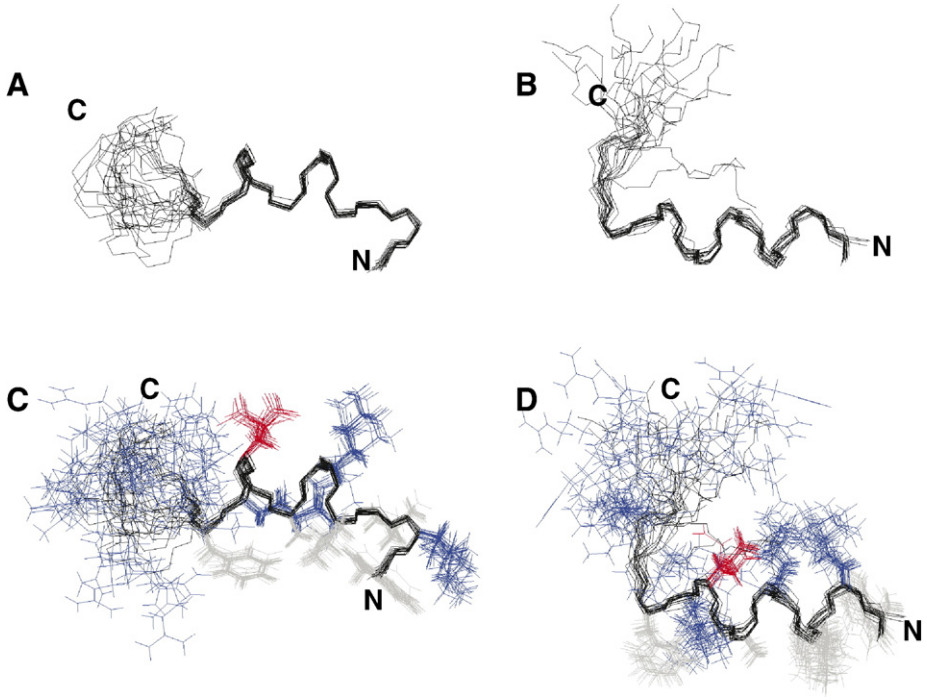

Fig. 5. Backbone traces of the 20 lowest energy structures of LFampinB bound to SDS (A) and DPC (B) micelles. (C) and (D) are in the same orientation as the figures above however, the hydrophobic amino acids, Trp, Leu, Ala and Phe, are colored gray; basic amino acids, Lys and Arg, have been colored blue; and the only negatively charged residue, Glu9, has been colored red. Note that in both structures, the side chains of Trp1 and Phe11 are oriented on the same face of the peptide and border what appears to be a hydrophobic patch. Most of the charged amino acids are found on the opposite side of this hydrophobic patch and contribute to the formation of an amphipathic structure. These figures were generated using MOLMOL [51] with the sets of structures fitted across the first 13 residues of LFampinB.

Table 2
Structural statistics for the NMR structures determined for LFampinB bound to SDS and DPC micelles

	SDS bound	DPC bound
No. of distance restraints		
Unambiguous NOEs	466	404
Ambiguous NOEs	18	15
Unassigned NOEs	2	2
Total NOEs	484	419
Broad Dihedral	15	15
RMSD from ideal values		
Bonds (Å)	$2.22\times10^{-3}\pm7.29\times10^{-5}$	$2.66\times10^{-3}\pm1.01\times10^{-4}$
Angles (degree)	$0.401\pm1.12\times10^{-2}$	$0.369\pm1.06\times10^{-2}$
Impropers (degree)	$0.253\pm1.71\times10^{-2}$	$0.190\pm2.28\times10^{-2}$
Van der Waals (kcal/mol)	15.01±0.61	10.51±1.66
Non-bonded energies		
Electronic (kcal/mol)	−437.03 (±49.00)	−491.15 (±42.61)
Van der Waals (kcal/mol)	−146.16 (±2.29)	−138.95 (±4.19)
Ramachandran space (%)[a]		
Most Favored	72.1	76.8
Additionally allowed	27.5	23.2
Generously allowed	0.4	0
Disallowed	0	0
Global RMSD (Å)[b]		
Backbone	0.741	0.577
Heavy	1.358	1.168

[a] Calculated by PROCHECK [52].
[b] Calculated by MOLMOL [51] using the first 13 residues of LFampinB from the 20 lowest energy structures obtained from the ARIA calculations.

The structural statistics for LFampinB in each membrane mimetic environment are shown in Table 2. The statistics for the Ramachandran space and the RMSD are based on the 20 lowest energy structures from the ARIA calculations using NOE distance restraints. The RMSD values have been calculated for the well-structured helical portion of the peptide and most of the unstructured C-terminus has not been taken into account for these values. Many of the backbone dihedral angles are found in the most favored or additionally allowed regions of the Ramachandran diagram and none of them are found in disallowed regions (Table 2).

Fig. 5 shows the backbone traces of LFampinB bound to micelles as well as charged and hydrophobic residues of the 20 lowest energy structures of the peptide in both lipid environments. The backbone and heavy atom RMSD for the structurally defined region of LFampinB, encompassing the first 13 residues, bound to SDS micelles is 0.741 Å and 1.358 Å, respectively. Examination of the SDS bound structure of LFampinB reveals a mostly helical structure between residues 1 and 11 (Fig. 5A). The cationic C-terminal region containing Lys13, Lys15 and Arg17 remains unstructured especially residues 15 and 17 (Fig. 5C). Gly12 follows the helix in LFampinB and it seems to initiate the flexibility of the C-terminal region.

A hydrophobic patch bordered by Trp1 and Phe11 is present in the SDS bound structure of LFampinB with the side chains of these aromatic residues both oriented in the same direction (Fig. 6A). Leu3, Leu4 and Ala7 are the other residues found in this region and they contribute to the hydrophobicity of this patch. The helical portion of LFampinB bound to SDS displays an amphipathic structure due to the charged face that lies opposite the hydrophobic patch. The positively charged residues in the helical region, namely Lys2, Lys6 and Lys10 are all oriented away from the hydrophobic patch (Fig. 6B). The only negatively charged residue in LFampinB is Glu9 whose charged side chain is oriented in the same direction as the positively charged Lys6 residue and could indicate a favorable ion-pair

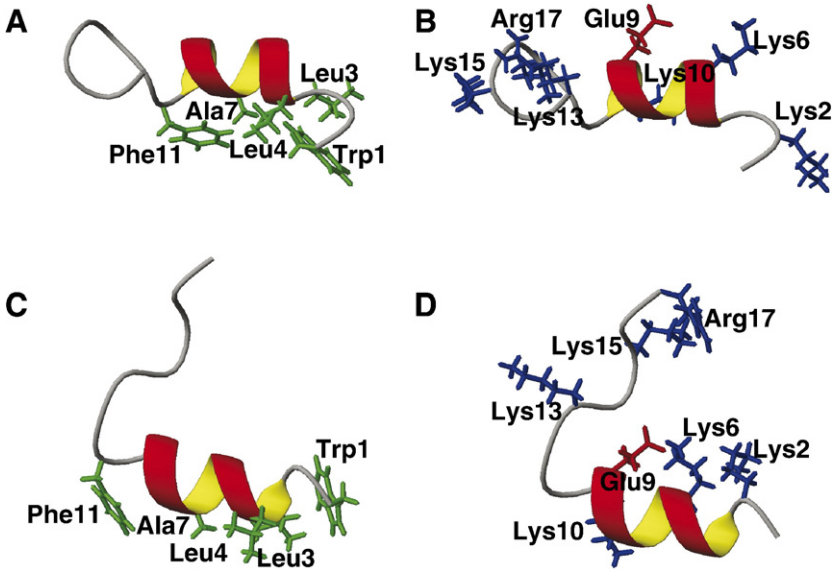

Fig. 6. Ribbon diagram of a representative structure of LFampinB bound to SDS (A and B) and DPC (C and D). In panel A, Trp1 and Phe11 are highlighted in green and they form the edges of a hydrophobic patch that also contains Leu3, Leu4 and Ala7. In panel B, the positively charged amino acids are shown in blue and are located opposite the hydrophobic patch or they are found in the unstructured C-terminus. The only negatively charged amino acid, Glu9, is colored red and is found as far away from the hydrophobic surface as possible. The same coloring scheme has been used for the DPC bound structure with the hydrophobic residues (C) and the charged residues (D) indicated. This figure was generated using MOLMOL [51].

(

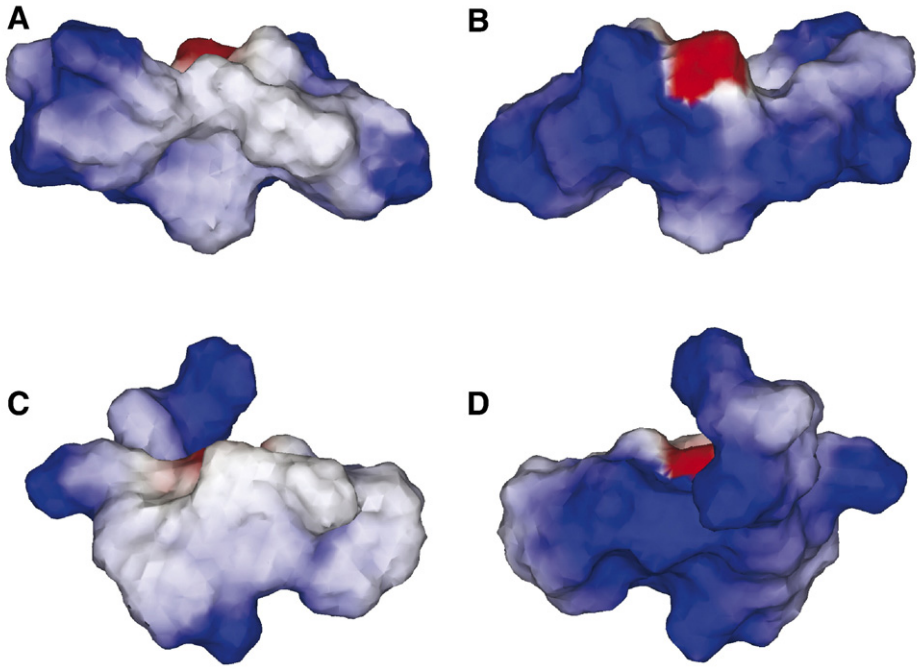

Fig. 7. Charge distribution on the surface of LFampinB bound to SDS (A and B) and DPC (C and D) micelles. Positively charged areas are shown in blue and the negatively charged residue, Glu9, is shown in red. In A and C the hydrophobic patch involving Trp1 and Phe11 is oriented toward the reader with Trp1 on the right hand side of each structure. B and D show the opposite face of the peptide and help to illustrate the amphipathic nature of LFampinB bound to micelles. These figures were generated using MOLMOL [51].

interaction between the opposing charges of these two residues (Fig. 6B).

The backbone and heavy atom RMSD for the DPC bound LFampinB structure are 0.577 Å and 1.168 Å respectively across the first 13 residues. We once again see good agreement between the NMR structures at the N-terminal portion of the peptide with the C-terminal residues being more disordered (Fig. 5B). Similar to the SDS bound structure, the hydrophobic amino acids orient themselves on one face of the peptide and positively charged residues are found opposite to this hydrophobic surface or in the unstructured C-terminus (Fig. 5D).

Upon closer examination of the structure of LFampinB bound to DPC, we see once again the formation of a helix across the first 11 residues of the peptide (Fig. 6C and D). Trp1 and Phe11 are found at the edges of a hydrophobic patch similar to that observed in the SDS bound structure (Fig. 6C). The Trp1 side chain appears to remain closer to the helix axis in the DPC bound structure compared to the SDS bound structure (Fig. 6C). The charged amino acid side chains are also found on the opposing face of this hydrophobic patch except for Lys10 which is found perpendicular to the hydrophobic patch (Fig. 6D).

4. Discussion

Determining the structure of an antimicrobial peptide can potentially provide insight into the mechanism used by the molecule to exert its antimicrobial effect. The predicted secondary structure of LFampinB indicates that the C-terminal residues of the peptide might be a random coil and examination of the corresponding stretch in the crystal structure of the intact bovine lactoferrin protein indicates that the C-terminal residues of LFampinB do not have regular secondary structure while the N-terminal residues form an α-helix [28]. A circular dichroism study of LFampinB suggested that the peptide contained both helical and flexible regions [15], however CD spectra cannot

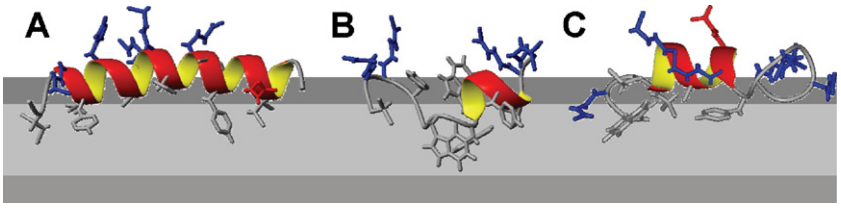

Fig. 8. Schematic representation of the interactions between magainin (A), tritrpticin (B) and LFampinB (C) and a lipid bilayer. Hydrophobic side chains have been colored gray. Positively charged residues are shown in blue and negatively charged residues are in red. The lipid bilayer is shown in the background. The head groups and the hydrophobic core are colored dark and light gray respectively. This figure was generated using MOLMOL [51].

assign this in a sequence specific manner. The solution structures of LFampinB bound to micelles presented here clearly show a flexible C-terminal region of the peptide with a well-defined N-terminal helix stretching from residues 1–11.

Both structures presented for LFampinB have a patch of hydrophobic residues on one face of the peptide (Fig. 5). The charged amino acid side chains are for the most part found opposite to this hydrophobic patch which gives lactoferrampin an amphipathic structure characteristic of other antimicrobial peptides derived from lactoferrin [2,29] and other sources [30]. However, a glycine scan of a slightly longer form of LFampinB, LFampin 265–284, has revealed the importance of the positively charged residues in the antimicrobial activity of LFampinB [31]. Substitution of five of the six positively charged residues in LFampinB led to a significant decrease in the antifungal activity of LFampin 265–284. The corresponding residues in LFampinB are Lys6, Lys10, Lys13, Lys15 and Arg17 and they all reside closer to the flexible end of LFampinB. The mutation of the residue corresponding to Lys2 in LFampinB to a glycine only had a minor effect on the antimicrobial activity of the peptide.

The importance of the cationic nature of antimicrobial peptides has been well documented [32,33]. It appears that LFampinB is capable of interacting with negatively charged membranes. The strongest fluorescence blue shift was observed in LUVs containing the negatively charged phosphatidylglycerol. This interaction could be due to the cationic charge of LFampinB which is favorably attracted to the negatively charged head groups of the ePG molecules. Many of the studies of LFampinB have focused on the candidacidal activity of this peptide [15,31,34]. The plasma membrane of *Candida* species contains a large proportion of negatively charged phospholipids, namely phosphatidic acid (PA) and phosphatidylglycerol [35]. In fact, the small head group on a PA molecule is similar to the small negatively charged head group of SDS, which also demonstrated a large blue shift in the fluorescence experiments. This could translate to a similar interaction between *Candida* plasma membranes and LFampinB. The decrease in fluorescence intensity observed when LFampinB interacted with SDS micelles is counter intuitive because if the tryptophan residue is binding to the micelle, there should be an increase in the intensity observed in the emission spectra. We have attributed the quenching of the tryptophan fluorescence in the presence of the SDS micelles to an interaction with the head groups of the detergent molecules. Our group has previously reported significant quenching of Trp fluorescence by sulfur atoms in methionine residues [36] and this might help explain the observed results because of the sulfur atom in the head group of the SDS molecules. However, the quenching of Trp fluorescence can involve many different pathways and mechanisms and we cannot be certain that this is the only factor contributing to the quenching of the emission from LFampinB in the presence of SDS.

Interestingly there is no significant blue shift in the presence of LUVs made from ePE:ePC or pure ePC. The lack of a blue shift in the presence of these zwitterionic phospholipids is understandable if electrostatic interactions mediate the initial binding of the peptide to the bilayer. The negative charges on the head groups of PG and SDS molecules could attract the positively charged LFampinB peptide followed by binding of Trp1 to the hydrophobic core of the membrane. In the case of the zwitterionic DPC micelles, it appears that Trp1 is capable of inserting into the hydrophobic core of the micelle despite the lack of an overall net negative charge to attract the positively charged peptide. This is attributed to a higher detergent concentration in the DPC micelles compared to the phospholipid concentration in the LUV samples, consequently pushing the equilibrium of LFampinB in the mixture to the membrane bound conformation. This is supported by the well-resolved NMR spectra that were acquired for LFampinB bound to DPC micelles, which allowed for the calculation of a well-defined peptide structure.

DSC has proven to be a valuable tool in examining interactions between antimicrobial peptides and lipids [37]. The DSC results support an electrostatic interaction between LFampinB and negatively charged phospholipids. The conversion from the lamellar gel phase to a rippled gel phase is what gives rise to the pretransition observed in DSC scans of lipid suspensions. This pretransition is due to interactions between the head groups of the lipid molecules and increasing the distance between the head groups through the insertion of a peptide eliminates these interactions and causes the pretransition peak to disappear [38]. The pretransition in DPPG bilayers disappears at high lipid:peptide ratios, indicating that LFampinB disrupts the head group organization in negatively charged DPPG MLVs. The main phase transition represents the conversion from the gel phase to a liquid crystal phase and is strongly influenced by the acyl chain packing of the phospholipid molecules [38]. Since there is no significant change in the main phase transition peak, it can be assumed that LFampinB does not significantly disrupt the acyl chain packing of the DPPG MLVs. There were no significant differences in the pretransition or the main phase transition of DPPC MLVs at various concentrations of LFampinB, indicating that the interactions between the peptide and membranes is head group dependant. The disappearance of the pretransition in DPPG MLVs has been observed for a 15-residue antimicrobial peptide derived from bovine lactoferricin with very little effect on the main phase transition. These peptides also demonstrated no effect on DPPC MLVs [39].

Tryptophan residues have the unique ability to reside at the lipid water interface of a plasma membrane [40] and their importance in antimicrobial peptides is well documented [11,13]. Many antimicrobial peptides contain one or more tryptophan residues and often they are key residues for determining activity [41]. Along with Phe11, Trp1 is found at the edge of a hydrophobic patch in LFampinB (Fig. 6A). The tryptophan fluorescence results demonstrate that the side chain of Trp1 becomes protected from the effects of a soluble quencher in the presence of a lipid micelle and vesicles with acidic head groups (Fig. 2) indicating that this residue preferentially inserts into the bilayer. Phenylalanine is a hydrophobic amino acid that is known to serve as a membrane anchor in transmembrane helices [42] as well as anchoring other antimicrobial peptides to the surface of a

plasma membrane [43]. The hydrophobic side chain of Phe11 side chain likely inserts into the hydrophobic core of the membrane and both of these residues serve to anchor LFampinB to the plasma membrane. This argument is more compelling considering that substitution of Trp1 with a glycine residue in LFampinB resulted in lower killing activity of the peptide [31] implying that this mutant was unable to bind to the surface of a plasma membrane.

The amphipathic nature of LFampinB is easily observed when the distribution of charges over the surface of the peptide is examined. The hydrophobic patch found in both the SDS-bound (Fig. 7A) and DPC-bound (Fig. 7C) structures of LFampinB is clearly visible. The opposite face of the hydrophobic surface contains most of the charged residues. It is also important to highlight the proximity of the negatively charged Glu9 to the nearby positively charged Lys6 in the SDS bound form of LFampinB (Fig. 7B). The repulsion effects between the acidic glutamate residue and the negatively charged bacterial membrane are mitigated by the proximity to the positively charged lysine residue and allow for the interaction of the hydrophobic patch with the membrane. In the DPC-bound structure, the negative charge from the glutamate side chain appears to be further away from any of the surrounding positive charges (Fig. 7D) likely because the charge repulsion between the peptide and the lipid is weaker in the presence of the zwitterionic micelle.

LFampinB and the longer form, LFampin 265–284, appear to act like a detergent and solubilize the plasma membrane of yeast and bacterial cells. Treatment of *C. albicans* and *E. coli* cells with LFampinB and LFampin 265–284 had large effects on plasma membrane integrity ranging from the formation of blebs to the appearance of vesicle like structures [34]. This has been described as the carpet model of membrane disruption as a mechanism of antimicrobial activity [44]. The amphipathic structure determined in this study lends support to this model of antimicrobial activity as do the tryptophan fluorescence and DSC studies. Once an effective concentration of LFampinB is reached, the hydrophobic patch on LFampinB inserts into the lipid bilayer and causes the plasma membrane to break apart leading to cell death.

It is useful to compare the micelle-bound structure of LFampinB to structures of other antimicrobial peptides. Magainin, the first linear antimicrobial peptide discovered from the skin of the African clawed frog [45] is relatively unstructured in aqueous solution. In the presence of lipids, magainin adopts a right-handed α-helical conformation that is amphipathic in nature [46,47]. The hydrophobic face of magainin preferentially inserts into the hydrophobic core of the lipid membranes and the positively charged face of the helix interacts with the negative head groups of the phospholipid bilayer (Fig. 8A). The amphipathic helix is a common motif observed in many other antimicrobial peptides [48] and the parallel orientation to the lipid bilayer normal has been found in other mammalian antimicrobial peptides. The human antimicrobial peptide LL-37 has been shown to reside in the interfacial region of a plasma membrane with the charged surface of the peptide interacting with the charged head groups of the lipids and the hydrophobic residues anchoring the peptide into the hydrophobic core of the bilayer [49]. The structures of LFampinB presented here represent a novel structural feature for helical antimicrobial peptides where the positively charged residues that are most important for the antimicrobial activity are flexible when bound to the membrane mimetic (Fig. 8C). Flexibility in the positively charged residues of an antimicrobial peptide has also been observed in tritrpticin where the arginine residues located at the N- and C-terminus of the peptide remain relatively unstructured while most of the non-polar residues contribute to the formation of a hydrophobic turn–turn structure that is thought to wedge into the center of the membrane [50] (Fig. 8B). However, most of the solution structures of helical amphipathic antimicrobial peptides reported to date demonstrate a well structured charged region of the peptide overlapping with the ordered hydrophobic portion of the peptide. The structures of LFampinB indicate that the positively charged residues at the C-terminus are required for its initial attraction to the negatively charged bacterial membrane surface but once the peptide binds, these residues do not appear to be directly involved in peptide binding to the membrane. This task is then taken over by the amphipathic helical portion of the peptide.

Acknowledgements

The authors would like to thank Dr. Deane McIntyre for his help with the NMR experiments, as well as Mr. Leo Nguyen for important discussions. The authors would also like to thank Dr. Elmar Prenner and Dr. Valery Andrushchenko for their assistance with the DSC experiments. HJV is the recipient of a Scientist award from the Alberta Heritage Foundation for Medical Research. The Bio-NMR center receives financial support from the Canadian Institutes for Health Research and the University of Calgary.

References

[1] W. Bellamy, M. Takase, K. Yamauchi, H. Wakabayashi, K. Kawase, M. Tomita, Identification of the bactericidal domain of lactoferrin, Biochim. Biophys. Acta 1121 (1992) 130–136.
[2] H.N. Hunter, A.R. Demcoe, H. Jenssen, T.J. Gutteberg, H.J. Vogel, Human lactoferricin is partially folded in aqueous solution and is better stabilized in a membrane mimetic solvent, Antimicrob. Agents Chemother. 49 (2005) 3387–3395.
[3] A. Pellegrini, U. Thomas, N. Bramaz, S. Klauser, R. von Fellenberg, Identification and isolation of a bactericidal domain in chicken egg white lysozyme, J. Appl. Microbiol. 82 (1997) 372–378.
[4] Y. Mine, F.P. Ma, S. Lauriau, Antimicrobial peptides released by enzymatic hydrolysis of hen egg white lysozyme, J. Agric. Food Chem. 52 (2004) 1088–1094.
[5] M.I.A. van der Kraan, J. Groenink, K. Nazmi, E.C.I. Veerman, J.G.M. Bolscher, A.V.N. Amerongen, Lactoferrampin: a novel antimicrobial peptide in the N1-domain of bovine lactoferrin, Peptides 25 (2004) 177–183.
[6] D. Caccavo, N.M. Pellegrino, M. Altamura, A. Rigon, L. Amati, A. Amoroso, E. Jirillo, Antimicrobial and immunoregulatory functions of lactoferrin and its potential therapeutic application, J. Endotoxin Res. 8 (2005) 403–417.
[7] J.L. Gifford, H.N. Hunter, H.J. Vogel, Lactoferricin: a lactoferrin-derived peptide with antimicrobial, antiviral, antitumor and immunological properties, Cell. Mol. Life Sci. 62 (2005) 2588–2598.

[8] L.T. Nguyen, D.J. Schibli, H.J. Vogel, Structural studies and model membrane interactions of two peptides derived from bovine lactoferricin, J. Pept. Sci. 11 (2005) 379–389.
[9] B.E. Haug, M.L. Skar, J.S. Svendsen, Bulky aromatic amino acids increase the antibacterial activity of 15-residue bovine lactoferricin derivatives, J. Pept. Sci. 7 (2001) 425–432.
[10] M.B. Strom, Ø. Rekdal, J.S. Svendsen, Antibacterial activity of 15-residue lactoferricin derivatives, J. Pept. Res. 56 (2000) 265–274.
[11] H.J. Vogel, D.J. Schibli, W.G. Jing, E.M. Lohmeier-Vogel, R.F. Epand, R.M. Epand, Towards a structure–function analysis of bovine lactoferricin and related tryptophan- and arginine-containing peptides, Biochem. Cell. Biol. 80 (2002) 49–63.
[12] J.P. Bradshaw, Cationic antimicrobial peptides — issues for potential clinical use, Biodrugs 17 (2003) 233–240.
[13] D.I. Chan, E.J. Prenner, H.J. Vogel, Tryptophan- and arginine-rich antimicrobial peptides: structures and mechanisms of action, Biochim. Biophys. Acta 1758 (2006) 1184–1202.
[14] S.R. Dennison, J. Wallace, F. Harris, D.A. Phoenix, Amphiphilic alpha-helical antimicrobial peptides and their structure/function relationships, Prot. Peptide Letters 12 (2005) 31–39.
[15] M.I.A. van der Kraan, K. Nazmi, A. Teeken, J. Groenink, W. van't Hof, E.C.I. Veerman, J.G.M. Bolscher, A.V.N. Amerongen, Lactoferrampin, an antimicrobial peptide of bovine lactoferrin, exerts its candidacidal activity by a cluster of positively charged residues at the C-terminus in combination with a helix-facilitating N-terminal part, Biol. Chem. 386 (2005) 137–142.
[16] D.J. Schibli, R.F. Epand, H.J. Vogel, R.M. Epand, Tryptophan-rich antimicrobial peptides: comparative properties and membrane interactions, Biochem. Cell. Biol. 80 (2002) 667–677.
[17] L.D. Mayer, M.J. Hope, P.R. Cullis, Vesicles of variable sizes produced by a rapid extrusion procedure, Biochim. Biophys. Acta 858 (1986) 161–168.
[18] F. Olson, C.A. Hunt, F.C. Szoka, W.J. Vail, D. Papahadjopoulos, Preparation of liposomes of defined size distribution by extrusion through polycarbonate membranes. Biochim. Biophys. Acta 557 (1979) 9–23.
[19] B.N. Ames, Assay of inorganic phosphate, total phosphate and phosphatases, in: E.F. Neufeld, V. Ginsberg (Eds.), Methods in Enzymology, Academic Press, New York, 1966, pp. 115–118.
[20] E.J. Prenner, R.N.A.H. Lewis, L.H. Kondejewski, R.S. Hodges, R.N. McElhaney, Differential scanning calorimetric study of the effect of the antimicrobial peptide gramicidin S on the thermotropic phase behavior of phosphatidylcholine, phosphatidylethanolamine and phosphatidylglycerol lipid bilayer membranes, Biochim. Biophys. Acta 1417 (1999) 211–223.
[21] J.R. Lakowicz, Principles of Fluorescence Spectroscopy, Kluwer Academic, New York, 1999.
[22] T.L. Hwang, A.J. Shaka, Water suppression that works. Excitation sculpting using arbitrary waveforms and pulsed field gradients, J. Magn. Reson. 112 (1995) 275–279.
[23] F. Delaglio, S. Grzesiek, G.W. Vuister, G. Zhu, J. Pfeifer, A. Bax, Nmrpipe — a multidimensional spectral processing system based on unix pipes, J. Biomol. NMR 6 (1995) 277–293.
[24] B.A. Johnson, R.A. Blevins, NMRView: a computer program for the visualization and analysis of NMR data. J. Biomol. NMR 4 (1994) 603–614.
[25] K. Wuthrich, NMR of Proteins and Nucleic Acids, John Wiley & Sons Inc., New York, 1986.
[26] A.T. Brunger, P.D. Adams, G.M. Clore, W.L. Delano, P. Gros, R.W. Grosse-Kunstleve, J.S. Jiang, J. Kuszewski, M. Nilges, N.S. Pannu, R.J. Read, L.M. Rice, T. Simonson, G.L. Warren, Crystallography and NMR system: a new software suite for macromolecular structure determination, Acta Crystallogr., D Biol. Crystallogr. 54 (1998) 905–909.
[27] J.P. Linge, M. Nilges, Influence of non-bonded parameters on the quality of NMR structures: a new force field for NMR structure calculation, J. Biomol. NMR 13 (1999) 51–59.
[28] S.A. Moore, B.F. Anderson, C.R. Groom, M. Haridas, E.N. Baker, Three-dimensional structure of diferric bovine lactoferrin at 2.8 angstrom resolution, J. Mol. Biol. 274 (1997) 222–236.
[29] P.M. Hwang, N. Zhou, X. Shan, C.H. Arrowsmith, H.J. Vogel, Three-dimensional solution structure of lactoferricin B, an antimicrobial peptide derived from bovine lactoferrin, Biochemistry 37 (1998) 4288–4298.
[30] J.P.S. Powers, R.E.W. Hancock, The relationship between peptide structure and antibacterial activity, Peptides 24 (2003) 1681–1691.
[31] M.I.A. van der Kraan, C. van der Made, K. Nami, W. van't Hof, J. Groenink, E.C.I. Veerman, J.G.M. Bolscher, A.V.N. Amerongen, Effect of amino acid substitutions on the candidacidal activity of LFampin 265–284, Peptides 26 (2005) 2093–2097.
[32] R.M. Epand, H.J. Vogel, Diversity of antimicrobial peptides and their mechanisms of action, Biochim. Biophys. Acta 1462 (1999) 11–28.
[33] K.A. Brogden, Antimicrobial peptides: pore formers or metabolic inhibitors in bacteria? Nat. Rev. Microbiol. 3 (2005) 238–250.
[34] M.I.A. van der Kraan, J. van Marle, K. Nazmi, J. Groenink, W. van't Hof, E.C.I. Veerman, J.G.M. Bolscher, A.V.N. Arnerongen, Ultrastructural effects of antimicrobial peptides from bovine lactoferrin on the membranes of *Candida albicans* and *Escherichia coli*, Peptides 26 (2005) 1537–1542.
[35] M. Abdi, D.B. Drucker, V. Boote, M. Korachi, E.D. Theaker, Phospholipid molecular species distribution of some medically important Candida species analysed by fast atom bombardment mass spectroscopy, J. Appl. Microbiol. 87 (1999) 332–338.
[36] T. Yuan, A.M. Weljie, H.J. Vogel, Tryptophan fluorescence quenching by methionine and selenomethionine residues of calmodulin: orientation of peptide and protein binding, Biochemistry 37 (1998) 3187–3195.
[37] K. Lohner, E.J. Prenner, Differential scanning calorimetry and X-ray diffraction studies of the specificity of the interaction of antimicrobial peptides with membrane-mimetic systems, Biochim. Biophys. Acta 1462 (1999) 141–156.
[38] B. Klajnert, J. Janiszewska, Z. Urbanczyk-Lipkowska, A. Bryszewska, R.M. Epand, DSC studies on interactions between low molecular mass peptide dendrimers and model lipid membranes, Int. J. Pharm. 327 (2006) 145–152.
[39] W.G. Jing, J.S. Svendsen, H.J. Vogel, Comparison of NMR structures and model–membrane interactions of 15-residue antimicrobial peptides derived from bovine lactoferricin, Biochem. Cell. Biol. 84 (2006) 312–326.
[40] W.M. Yau, W.C. Wimley, K. Gawrisch, S.H. White, The preference of tryptophan for membrane interfaces, Biochemistry 37 (1998) 14713–14718.
[41] M.B. Strom, B.E. Haug, Ø. Rekdal, M.L. Skar, W. Stensen, J.S. Svendsen, Important structural features of 15-residue lactoferricin derivatives and methods for improvement of antimicrobial activity, Biochem. Cell. Biol. 80 (2002) 65–74.
[42] A.B. Meijer, R.B. Spruijt, C.J.A.M. Wolfs, M.A. Hemminga, Membrane-anchoring interactions of M13 major coat protein, Biochemistry 40 (2001) 8815–8820.
[43] X. Li, Y. Li, A. Peterkofsky, G.S. Wang, NMR studies of aurein 1.2 analogs, Biochim. Biophys. Acta 1758 (2006) 1203–1214.
[44] Z. Oren, Y. Shai, Mode of action of linear amphipathic alpha-helical antimicrobial peptides, Biopolymers 47 (1998) 451–463.
[45] M. Zasloff, Magainins, a class of antimicrobial peptides from Xenopus skin — isolation, characterization of 2 active forms, and partial cDNA sequence of a precursor, Proc. Natl. Acad. Sci. U. S. A. 84 (1987) 5449–5453.
[46] B. Bechinger, Structure and functions of channel-forming peptides: magainins, cecropins, melittin and alamethicin, J. Membr. Biol. 156 (1997) 197–211.
[47] J. Gesell, M. Zasloff, S.J. Opella, Two-dimensional H-1 NMR experiments show that the 23-residue magainin antibiotic peptide is an alpha-helix in dodecylphosphocholine micelles, sodium dodecylsulfate micelles, and trifluoroethanol/water solution, J. Biomol. NMR 9 (1997) 127–135.
[48] A. Tossi, L. Sandri, A. Giangaspero, Amphipathic, alpha-helical antimicrobial peptides, Biopolymers 55 (2000) 4–30.
[49] U.H.N. Durr, U.S. Sudheendra, A. Ramamoorthy, LL-37, the only human member of the cathelicidin family of antimicrobial peptides, Biochim. Biophys. Acta 1758 (2006) 1408–1425.
[50] D.J. Schibli, P.M. Hwang, H.J. Vogel, Structure of the antimicrobial peptide tritrpticin bound to micelles: a distinct membrane-bound peptide fold, Biochemistry 38 (1999) 16749–16755.
[51] R. Koradi, M. Billeter, K. Wuthrich, MOLMOL: a program for display and analysis of macromolecular structures, J. Mol. Graph. 14 (1996) 51–55.
[52] R.A. Laskowski, J.A. Rullmann, M.W. MacArthur, R. Kaptein, J.M. Thornton, AQUA and PROCHECK-NMR: programs for checking the quality of protein structures solved by NMR, J. Biomol. NMR 8 (1996) 477–486.